ACS Biomaterials SCIENCE & ENGINEERING

Article

pubs.acs.org/journal/abseba

Graphene Foam as a Three-Dimensional Platform for Myotube Growth

Eric Krueger,[†,‡] A. Nicole Chang,[†] Dale Brown,[†] Josh Eixenberger,[§,⊥] Raquel Brown,[§] Sepideh Rastegar,[∥] Katie M. Yocham,[#] Kurtis D. Cantley,[∥] and David Estrada*[,†]

[†]Micron School of Materials Science and Engineering, [§]Biomolecular Research Center, [⊥]Physics Department and Biomolecular Sciences Doctoral Program, [∥]Department of Electrical and Computer Engineering, and [#]Department of Mechanical and Biomedical Engineering, Boise State University, 1910 University Drive, Boise, Idaho 83725, United States

Supporting Information

ABSTRACT: This study demonstrates the growth and differentiation of C2C12 myoblasts into functional myotubes on three-dimensional graphene foam bioscaffolds. Specifically, we establish both bare and laminin-coated graphene foam as a biocompatible platform for muscle cells and identify that electrical coupling stimulates cell activity. Cell differentiation and functionality is determined by the expression of myotube heavy chain protein and Ca^{2+} fluorescence, respectively. Further, our data show that the application of a pulsed electrical stimulus to the graphene foam initiates myotube contraction and subsequent localized substrate movement of over 100 μm. These findings will further the development of advanced three-dimensional graphene platforms for therapeutic applications and tissue engineering.

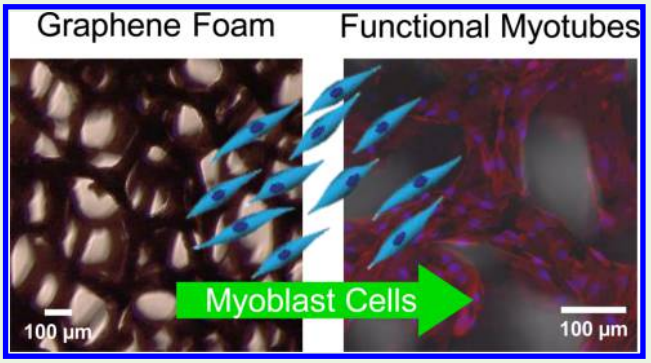

KEYWORDS: *graphene foam, C2C12, extracellular matrix, tissue engineering scaffold, confocal microscopy, X-ray micro-CT*

INTRODUCTION

The transition from traditional two-dimensional (2D) cell culture platforms toward three-dimensional (3D) systems seeks to overcome the limitations of 2D cellular models and mimic the native cellular microenvironment. Such 3D tissue culture platforms provide the opportunity for further understanding of structure−function relationships and tissue pathophysiology; as well as facilitate the development of novel regenerative medical treatments to help restore and strengthen lost functionality.[1−3] A critical challenge of this evolution has been the development of biocompatible scaffolding to simulate the natural extracellular matrix (ECM). Beyond the biological materials such as protein-based ECMs, novel engineered materials offer improved functionality and customization for localized chemical delivery and bioactivity monitoring.[1] Among these materials, graphene has become an excellent alternative because of its physical, electrical, and mechanical properties.[4]

Numerous investigations on graphene and its derivatives have established it as an excellent substrate for cell culture.[5−9] Its favorable hydrophobicity characteristics,[5,10] propensity for serum protein adsorption[7] and potential for integrated electrochemical sensing[11] provide graphene with remarkable attributes for an advanced cell growth platform. However, being an atomically thin 2D material, planar graphene has limited surface area with which to establish a cell−substrate interface. Graphene foam (GF) is a 3D analog of planar graphene that shares many of the same favorable physical and electrical characteristics,[12] but is fabricated as a porous scaffold, significantly increasing the surface area available for cell growth. GF has already found use in battery and supercapacitor technology and has exhibited potential for hydrophobic coating and filtering applications.[13−16] Additionally, GF is rapidly emerging as a platform for advanced biomedical, biosensing, and tissue engineering therapies[17−19] and has already been demonstrated as a biocompatible platform for neural cell growth, osteogenic differentiation, and chondrogenic differentiation.[17,20,21] However, the use of graphene foam as a conductive 3D scaffold for muscle tissue remains unreported. Such a demonstration would show that graphene foam is a suitable platform for growth of the major components of the musculoskeletal system, while providing a platform to electrically interface with engineered muscle tissue for a variety of applications in tissue models and bio hybrid systems.[22]

In this work, we investigate the culture of C2C12 murine myoblast cells on 3D graphene foam grown by chemical vapor deposition (CVD), and explore its feasibility as a platform for functional muscle cell growth. Using immunostaining and confocal microscopy, we identify the growth and differentiation of C2C12 cells into functional myotubes on both bare and laminin-coated GF. We find that the cells conform to the

Received: March 10, 2016
Accepted: June 24, 2016
Published: June 24, 2016

DOI: 10.1021/acsbiomaterials.6b00139
ACS Biomater. Sci. Eng. 2016, 2, 1234−1241

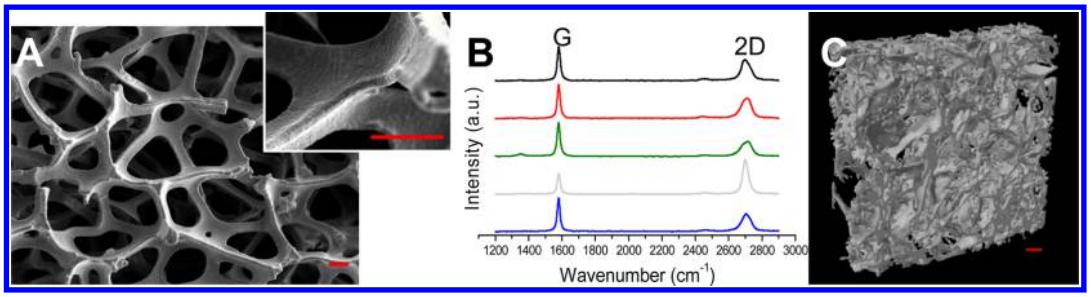

Figure 1. Characterization of GF. (A) SEM image of GF. (inset) Increased SEM magnification reveals the surface characteristics of the GF. (B) Raman spectra indicating our growth parameters result in multilayer graphene comprising the foam. (C) Micro-CT scan of GF reveals the internal structural characteristics. Scale bars: 100 μm.

structural contours of the scaffold and express myosin heavy chain (MHC) suggesting their differentiation into myotube cells. Our work represents fundamental research into the use of GF as an electrically active three-dimensional platform for muscle cell growth.

MATERIALS AND METHODS

Graphene Foam Growth and Characterization. GF was grown on 1.2 mm thick nickel (Ni) foam in a custom built CVD system. The nickel foam was annealed for 60 min under Ar/H_2 flow and graphene was grown under a CH_4/H_2 flow at 1000 °C for 10 min at a pressure of ~200 mTorr. The resulting Ni/graphene foam substrates were cooled to room temperature under Ar/H_2 gas flow and etched in $FeCl_3$ for 24 h to remove the Ni. The resultant free-standing graphene foam was rinsed with DI water before characterization (Figure S1).

The GF was imaged with scanning electron microscopy (Hitachi S-3400N−II, Tokyo, Japan) and analyzed with Raman spectroscopy (HORIBA Instruments Inc., Edison, NJ) to determine the structural composition of the foam. The graphene foam was also imaged and analyzed with a SkyScan 1172 (Bruker MicroCT, Kontich, Belgium) demonstrating GFs compatibility with advanced 3D medical imaging techniques.

All of the GF samples used for cell culture were grown from the same large Ni foam scaffold to ensure a consistent cell growth surface area. Prior to cell culture, GF samples were sterilized in 70% ethanol and washed with sterile DPBS buffer. One-half of the samples were then incubated in 10 μg/mL laminin solution at 8 °C overnight. Excess laminin solution was aspirated and the samples were then washed with sterile DPBS. All GF samples were incubated in Dulbecco's Modified Eagle Medium (DMEM), (Life Technologies; Carlsbad, CA) with 10% (v/v) fetal bovine serum (FBS), (Life Technologies, Carlsbad, CA) and 1% penicillin/streptomycin (Life Technologies, Carlsbad, CA) growth media (GM) in 5% CO_2 at 37 °C overnight before cell seeding.

Cell Culture. C2C12 (ATCC CRL-1772) myoblast cells (ATCC, Manassas, VA) were cultured in GM in 5% CO_2 at 37 °C. Each GF sample was seeded with approximately 45,000 cells and incubated in 5% CO_2 at 37 °C. After 24 h, the media was changed to differentiation media (DM) containing DMEM, 2% (v/v) horse serum (Life Technologies, Carlsbad, CA), 1% penicillin/streptomycin and 50 ng/mL Insulin-like Growth Factor-1 (IGF-1), (Sigma-Aldrich, St. Louis, MO). The DM was exchanged every 2 days when applicable. After growth and differentiation, the cells were fixed with a solution of 2% paraformaldehyde, and the GF samples were transferred to a glass-bottom Petri dish.

X-ray Computed Microtomography (MicroCT). Graphene foam samples were scanned with a SkyScan 1172 (Bruker MicroCT, Kontich, Belgium). Briefly, graphene foam samples were transferred from solution, mounted onto a small filter and allowed to dry fully overnight. The GF/filter was placed upright on the *z*-axis of the sample holder, centered and secured to eliminate scan artifacts due to random movement. Scan data was acquired with an X-ray tube setting of 23 kV, 127 μA, and an exposure time of 2700 ms; scan parameters for the 180°scan were defined with a step size of 0.3 degrees, ten-frame averaging and a pixel size of 2.56 μm. Cross section images were reconstructed from the shadow projections utilizing NRecon software (version 1.6.10.4) based on the Feldkamp algorithm. SkyScan CT Analyzer (CTan) software (version 1.15.4.0) was utilized to perform quantitative analysis and generate 3D models: GF object volume, structure thickness and surface area were calculated based on 3D models generated using the Adaptive rendering algorithm after binarization of the reconstructed slices.

Immunofluorescence. Cells were permeabilized and blocked with 0.1% Triton X-100 (Sigma-Aldrich, St. Louis, MO) and BlockAid (Life Technologies, Carlsbad, CA), respectively, then incubated overnight at 8 °C with a primary antibody specific to sarcomere myosin (MHC): MF-20 (Developmental Studies Hybridoma Bank, University of Iowa, Iowa City, Iowa). Secondary labeling of the MF-20 was performed with a goat antimouse antibody tagged with Alexa Fluor 488 (Life Technologies, Carlsbad, CA) In addition, the cells were labeled for cytoskeletal F-actin with Alexa Fluor 546 conjugated to phalloidin, counterstained with Hoechst for DNA, and mounted with ProLong Gold (Life Technologies, Carlsbad, CA). Samples were allowed to cure overnight before imaging.

Confocal Imaging. Samples were imaged with the Zeiss LSM 510 Meta system combined with the Zeiss Axiovert Observer Z2 inverted microscope and ZEN 2009 imaging software (Carl Zeiss, Inc., Thornwood, NY). Confocal Z-stack images were acquired utilizing the Plan-Apochromat 20x/NA 0.8 and Fluar 40x/NA 1.30 Oil objectives and with three laser sources: diode (405 nm), an argon (488 nm) and HeNe (543 nm). Transmitted light was also collected on one channel during the Z-stack acquisition to provide contrast to the GF structure. Image processing was performed with ZEN 2009 imaging software (Carl Zeiss, Inc., Thornwood, NY) and ImageJ.[23]

Electrical Stimulation. C2C12 cells were cultured on GF as described then transferred to a new sterile dish to eliminate background fluorescence from cells not adhered to foam. The samples were incubated for 1 h at 37 °C in DM containing 5 μM Fluo-4 AM (Life Technologies, Carlsbad, CA). The cells were then washed with fresh warm DM and incubated for 30 min at 37 °C. The sample was oriented between 2 Pt electrodes arranged 1 cm apart. One electrode was placed in direct contact with the foam sample. A biphasic square pulse train was applied to the sample (±10 V, 50 ms, 1 Hz)[5,24] and the subsequent cell response was imaged with the Zeiss LSM 510 configured for epifluorescence time-lapse imaging. The increase in fluorescence intensity was determined by comparing the intensity values of pixels during cell stimulation and at rest (no applied stimulus). Image processing and tracking was performed with ImageJ[23] and the MTrackJ plugin.[25]

RESULTS

Graphene Foam Growth and Characterization. Graphene was grown by CVD on a nickel foam scaffold and imaged with scanning electron microscopy (SEM) (Figure 1A). The SEM micrograph shows the porous structure and micro-structural channels of the GF, and the inset further reveals the

DOI: 10.1021/acsbiomaterials.6b00139
ACS Biomater. Sci. Eng. 2016, 2, 1234−1241

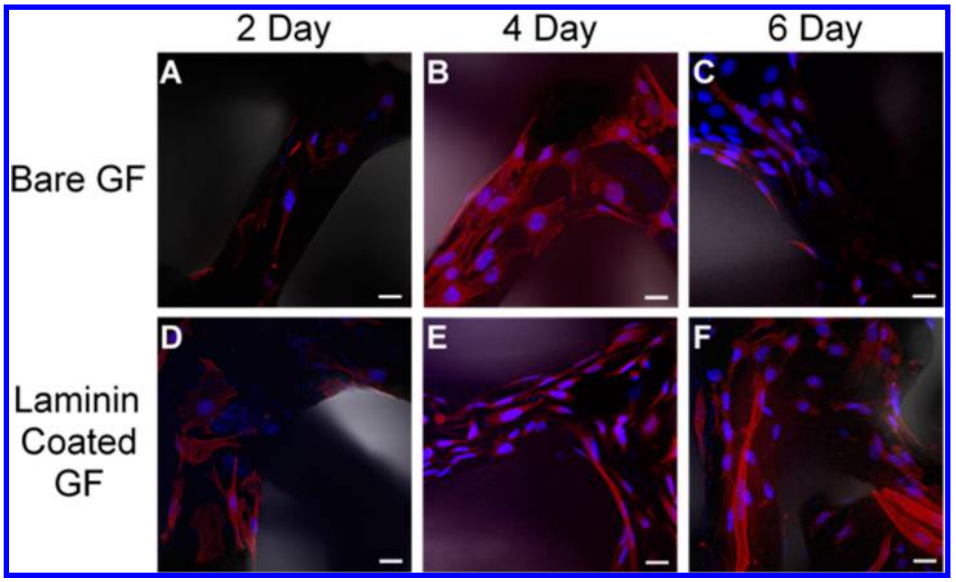

Figure 2. Representative confocal Z-stack images of C2C12 cells cultured on GF. Blue, nuclei (Hoechst); red, actin (Alexa Fluor 546 phalloidin). Growth on bare GF after culture in DM for (A) 2, (B) 4, and (C) 6 days. Laminin-coated GF after culture in DM for (D) 2, (E) 4, and (F) 6 days. Scale bars: 20 μm.

wrinkles of the graphene as it adheres to the structure of the Ni foam.

After etching, the free-standing graphene foam was characterized with Raman spectroscopy to identify the number of graphene layers (Figure 1B). The Raman spectra exposes the characteristic G (~1585 cm^{-1}) and 2D peaks (~2700 cm^{-1}) typical of graphene. The absence and/or low intensity of the characteristic D peak (~1350 cm^{-1}) indicates the GF has a low defect density. To further characterize the structure of the GF for cell growth, we analyzed the sample using micro-CT and determined a comprehensive structural depiction of the scaffold (Figure 1C). From the scans, the GF was calculated to have a surface area to volume ratio of 323.34 mm^{-1}, an object volume to total volume ratio (Obj.V/TV) of 16.44% corresponding to a porosity of 84.56%, and an average structure thickness (St.Th) of 10.57 μm ± 3.8 μm.

The microscale and macroscale mechanical properties of GF have previously been investigated with nanoindentation and in situ tensile strength testing, respectively.[26] Nieto et al. used commercially procured (Graphene Laboratories) CVD synthesized free-standing GF with typical pore sizes of 100−200 μms in diameter, produced with parameters similar to those in this study. Hydrogen and methane were introduced into a furnace that heats to 1000 °C to grow graphene on nickel foam, and the nickel was foam was etched away postgrowth. Nanoindentation revealed low GF hardness (19.9−26.1 kPa) and elastic modulus (1.2−1.5 MPa). Tensile testing showed the elastic modulus of bulk GF to be higher (69.9 GPa) because of the alignment of the graphene branches. Engler et al. previously reported the ideal modulus of elasticity for C2C12 differentiation as ~12 kPa for maximum myosin striations; C2C12 cells did not striate on much stiffer substrates.[27]

Assessing Laminin Coating on Cell Growth. A large GF sample was divided into smaller pieces to compare cell growth between samples coated with laminin and uncoated samples. Many reports evaluating cell growth and differentiation utilize quantitative assessment tools such as fusion index.[28−30] However, the fusion index technique requires characterizing cells in discrete planar regions, an aspect that is not feasible with 3D cell culture. Consequently, we quantified the myoblast and myotube densities after fixing and staining the cells by counting the number of nuclei and estimating the scaffold surface area. This permitted us to make approximate comparisons of cell growth and differentiation between the laminin-coated and uncoated GF samples.

After 2 days in DM, both the laminin-coated GF samples and the uncoated (bare GF) had observable cell growth demonstrating the feasibility of both scaffolds for C2C12 attachment (Figure 2A, D). Both substrates exhibited regions of higher cell densities (Figure S2A, B); however, there was only a ~ 2% difference in average cell density after 2 days of growth (Figure 3A) suggesting that the seeding density was approximately the same between samples. We note that not all seeded cells adhere to the GF, as the pore size in the foam allows cells to drift to the bottom of the cell culture dish (Figure S3). The cells grown on the laminin coated GF (Figure 2D) exhibit a much more elongated structure after 2 days, suggesting their emergent differentiation into myotube cells.[31]

After 4 days, both preparations of GF samples exhibit extensive cell growth (Figures 2B, E). The cell density on the laminin-coated substrate was ~30% larger than on the bare GF (Figure 3A), and also appear more elongated with multinucleated cell structures suggesting myotube differentiation.[31,32] Additional images of 4-day cultures on bare and laminin-coated GF are available in the Figure S2B, D. After 6 days, both samples exhibit multinucleated myotube formation (Figure 2C, F). However, the estimated cell density of the bare GF was ~26% greater than the laminin-coated scaffold (Figure 3A). We attribute this unexpected discrepancy to the inaccuracies in quantifying the cell density from the confocal images. The 3D cell culture platform also hinders an accurate quantitative assessment of cell fusion and morphology for assessing myotube differentiation; therefore, we used immunofluorescence to identify cell differentiation.

C2C12 Differentiation. C2C12 myoblast cells are known to express the protein myosin heavy chain (MHC) upon their differentiation into myotube cells. Using immunofluorescence, we labeled MHC to further identify and analyze the cell

DOI: 10.1021/acsbiomaterials.6b00139
ACS Biomater. Sci. Eng. 2016, 2, 1234−1241

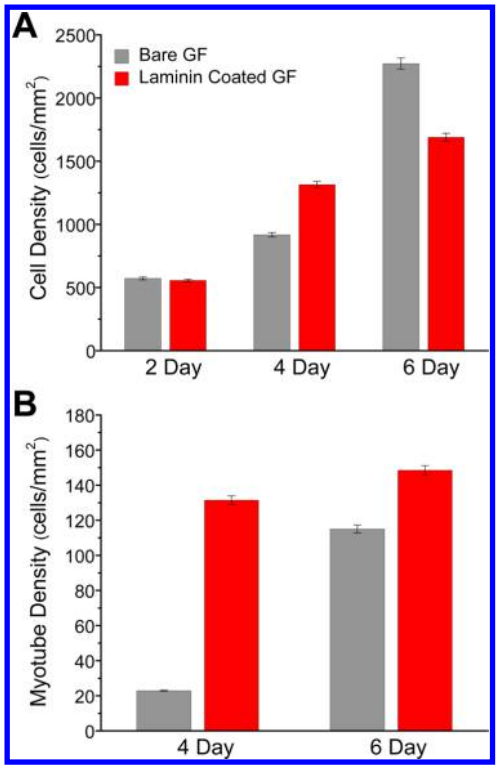

Figure 3. (A) Cell density determined from the number of nuclei and estimated surface area for cultures on bare and laminin coated GF after 2, 4, and 6 days. The error bars are the propagated errors from calculating the growth area. (B) Myotube density determined from multinucleated and MHC expressing cells and the estimated surface area for cultures on bare and laminin-coated GF. No myotube differentiation was observed after 2 days on either substrate. The error bars are the propagated errors from calculating the growth area.

differentiation on bare and laminin coated GF substrates. Although the MHC fluorescence imaging was performed during the same confocal scans as the actin and nuclei imaging, the MHC images are separated from Figure 2 for clarity. Images displaying the cell structure (Figure 2) combined with MHC fluorescence are provided in Figure S4.

After 2 days, the bare GF samples reveal some small and irregular fluorescent areas (Figure 4A), but these regions are more likely due to nonspecific binding of the antibodies since these small globular features were observed in all of the samples. To confirm this observation, we characterized the myotube density using the same estimated GF surface area used for myoblast cell density. We required a myotube to be positive for MHC expression as indicated by immunofluorescence and be multinucleated. C2C12 cells are known to express MHC before fusion into myotubes,[33] so immunofluorescence alone may not be a comprehensive indicator. After 2 days of growth, we found no myotube formation on either GF preparation meeting our criteria. After 4 days, only slight regions of fluorescence are observed (Figure 4B), but they appear to follow the contours of the cells suggesting emergent differentiation. After 6 days, several cells exhibit MHC fluorescence (Figure 4C) indicating that bare GF can be used as a substrate for C2C12 differentiation. By contrast, the cells grown on the laminin-coated GF exhibited greater numbers of differentiated cells. After 2 days, we observed cells that are expressing MHC as indicated by immunofluorescence (Figure 4D). However, those cells remain mononucleated and were not considered myotubes. After 4 days, we observe myotubes on the laminin coated substrates (Figure 4E), but identified only one myotube on all of the bare GF samples. Both substrate preparations yielded myotube growth after 6 days (Figure 4C, F), but the laminin coated GF had a ~22% greater myotube density (Figure 3B).

Assessing Cell Functionality. Although the cell differentiation was verified by immunofluorescence, cell functionality remained to be demonstrated. The usefulness of GF as a cell growth scaffold relies on the ability of cells to become functional muscle cells that could be used for contraction. As myotubes, C2C12 cells are electrically active and have been shown to respond to applied electrical stimulus.[5,24,34−36] Previous reports have used fluorescent Ca^{2+} imaging to identify

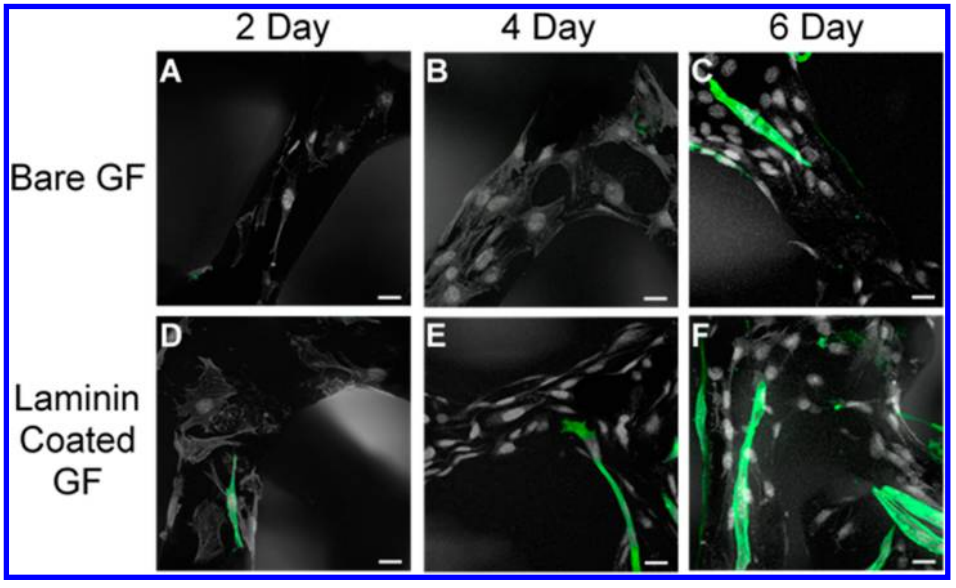

Figure 4. Immunofluorescence of MHC indicative of C2C12 differentiation. Green, MF-20 (Alexa Fluor 488 goat antimouse). Differentiation of C2C12 grown on bare GF for (A) 2, (B) 4, and (C) 6 days. Differentiation of C2C12 grown on laminin-coated GF for (D) 2, (E) 4, and (F) 6 days. Scale bars: 20 μm.

DOI: 10.1021/acsbiomaterials.6b00139
ACS Biomater. Sci. Eng. 2016, 2, 1234−1241

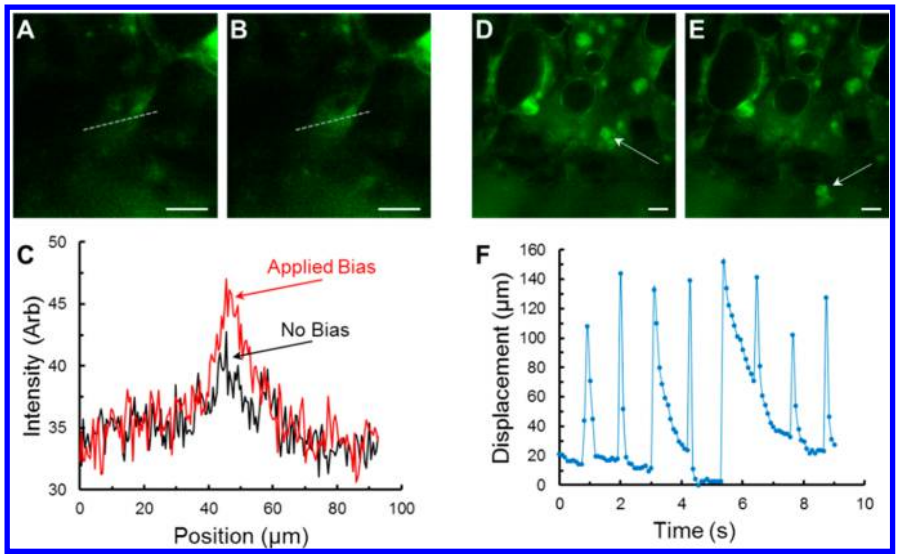

Figure 5. Fluorescence of C2C12 cells labeled with Fluo-4 AM during electrical stimulation. (A) Fluorescence intensity before and (B) during an applied electrical pulse. (C) Change in fluorescence intensity along a profile of a representative labeled myotube. Path of intensity profile is along the dotted line shown in A and B. (D, E) Sequential fluorescence images demonstrating the change in position of a region of the sample during a single electrical pulse. (F) Cyclic displacement of a region of the sample from an applied pulse train. Scale bars: 50 μm.

C2C12 functionality as well as studies with neural cells on GF.[21] By identifying changes in fluorescence intensity and position triggered by a series of voltage pulses, we reveal the functionality of differentiated myotube cells on GF.

Differentiated cells on GF were labeled with Fluo-4 AM calcium indicator and pulsed by a biphasic voltage train (±10 V, 50 ms duration, 1 Hz) with Pt electrodes in electrical contact with the GF (Figure S5). With the application of an electrical pulse, an increase in fluorescence intensity was observed along the myotube structures. To analyze the increase in fluorescence, we extracted a cross-sectional intensity profile from a representative region of cells before (Figure 5A) and during (Figure 5B) electrical stimulation. Analysis of the fluorescence intensity revealed a ∼10% increase in the fluorescence indicating a cellular response to the stimulus (Figure 5A). More interestingly, the series of electrical pulses stimulated contraction of the cells resulting in the motion of the GF substrate (Movies S1 and S2). To analyze the observed stimulative response, we captured the motion of a small region of GF in a time-lapse series of images. The piece of GF indicated by the arrows in two sequential images (Figure 5D, E) demonstrates the changes in the position of the representative region before and after electrical stimulation, respectively. The motion of the region was tracked frame-by-frame and the relative displacement was analyzed as a function of time (Figure 5F).

The motion is in phase with the pulse frequency and changes in the pulse frequency (500 mHz) resulted in changes in the frequency of cell contraction (not shown). Motion analysis reveals that the region has not always returned to the original position before the succeeding pulse is applied. This piece of the GF is one of the uncoupled distal ends on the outer scaffold structure which yields a greater range of motion than other surrounding connected pieces. However, from the time-lapse movies (Movies S1 and S2), it is clear that other regions of the GF with cells also exhibit motion during stimulation. No motion was detected when regions of GF without cells were subjected to electrical stimulation; this suggests the contraction of the stimulated cells is the source of the movement. Some of the GF pores shown in Figure 5 and in the movies have visible bubbles lodged in them. Because these bubbles were not present during cell growth, we suspect that they occurred during the transfer, labeling, and washing steps immediately prior to the electrical stimulus and imaging and do not interfere with the electrical stimulation.

DISCUSSION

The GF takes the shape of the nickel-foam scaffold used during fabrication. When seeding cells for culture, the porous nature of the foam means that many cells fall onto the substrate below (Figure S3). The cells that adhere and grow on the GF were those that remain in the scaffold after seeding. It is possible that the enhanced growth and differentiation on the laminin coated substrates is a consequence of the ease by which the cells adhere to the substrate, which has been demonstrated to influence proliferation.[37,38]

As described in the Methods section, the graphene foam was incubated in a solution of laminin, then rinsed with PBS. Any remaining laminin was assumed to only coat the GF in a thin layer. The thickness of the laminin coating has been previously estimated to be on the order of a nanoscale coating,[39,40] so any decrease in the pore size of the GF would be negligible. Therefore, we presume the enhanced cell growth of the laminin coated GF is due to differences in surface characteristics, not from being physically ensnared in the foam "net" during seeding. Surprisingly, the bare GF acted as a suitable growth substrate. Comparing the cell growth on either scaffold, cells on the laminin-coated GF demonstrated an increased differentiation at any given time, but the coating may have only increased the rate of differentiation. Comparing the representative images in of MHC fluorescence, it appears that the laminin-coated GF cell culture has differentiated more quickly.

Compared to C2C12 cells cultured on planar graphene, the GF samples exhibited larger cell and myotube densities after the same period of time. The cell density of C2C12 cells for planar graphene has been reported to be 950 cell mm^{-2} after 4 days.[5] After 4 days on GF, the average cell density was 917 cell mm^{-2} for bare GF and 1314 cell mm^{-2} on laminin-coated GF.

DOI: 10.1021/acsbiomaterials.6b00139
ACS Biomater. Sci. Eng. 2016, 2, 1234−1241

Although the planar graphene and GF substrates were initially seeded with the same number of C2C12 cells, the actual number of cells seeded on the GF was much lower because many cells fell through the porous substrate. Additionally, analysis of the myotube density to compare the 2D and the 3D graphene substrates yields 36 myotube per mm^{-2} for the planar graphene and 131 myotubes per mm^{-2} on the laminin-coated GF after 4 days. The bare GF substrates did not have enough myotubes for a meaningful analysis after 4 days. Nonetheless, these results still demonstrate that the increased surface area of the 3D culture scaffold is capable of supporting larger numbers of functional muscle cells.

The myotubes on the planar graphene surface, however, were much larger than those on the GF. Analysis of the myotube size shown in Reference5 reveal an average length of 602 ± 117 μm and width of 26 ± 3 μm. The myotubes on the laminin coated GF had an average length of 144 ± 38 μm and width of 6 ± 3 μm (Figure 6A, B). The large variation in length and width we

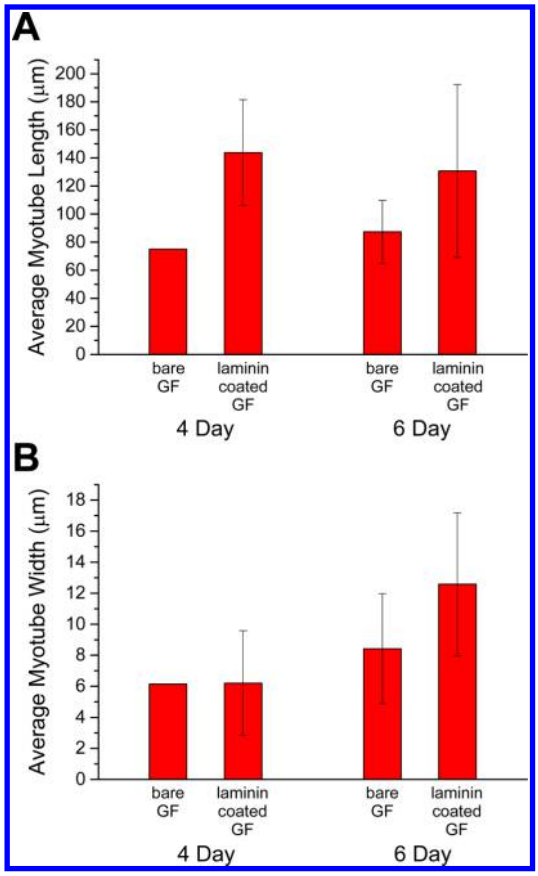

Figure 6. (A) Average myotube length for bare and laminin-coated GF after 4 and 6 days. The error bars are the standard deviation in the length. (B) Average myotube width for bare and laminin coated GF after 4 and 6 days. The error bars are the standard deviation in the width.

can attribute to the difficulty of analyzing cells grown on a 3D substrate. The longer myotubes follow the contours of the GF and are consequently partially hidden by the scaffold. Many of the myotubes can only be analyzed by measuring their thickness instead of their width. Cross-sectional analysis of C2C12 cells grown with IGF-1 has demonstrated that myotube width increases, but their thickness does not.[41] These limitations may be overcome by a more advanced analysis with micro-CT, but the optimization of that technique for quantifying cell growth and differentiation is beyond the scope of this work.

Although GF substrate remained in physical contact with the fixed Pt electrodes, its flexibility still permitted significant cell movement during the stimulus. The cells were seeded on the GF simply by adding the stock cell solution over the sample. In this study, no effort was made to align the cells or direct their growth in a particular direction. As a result, the cells simply follow the contours of the GF structure and do not appear to have a preferential direction of growth, a characteristic that would be favorable for structural muscle. Given the random nature of the GF structure, further evaluation of growth direction using analysis such as fast Fourier transform (FFT) analysis would not be practical for this investigation of 3D structural growth.

Previous work has demonstrated that the matrix elasticity plays a significant role in stem cell lineage specification, just as soluble induction factors can.[42] Deeper investigations into this study of C2C12 differentiation on GF could involve further characterization of the mechanical properties of the substrate. Evaluations of change in differentiation ability as a function of the stiffness of GF could validate and enhance previous conclusions demonstrating that myotubes differentiate optimally on substrates with tissuelike stiffness.[27]

CONCLUSIONS

We have demonstrated the feasibility of GF as a 3D scaffold for functional myotube growth. Although GF has also shown promise for use with other cell lines, its electrochemical characteristics are ideally suited for electrically active structural cells such as myotubes. We found that although laminin coating enhanced cell proliferation, it was not critical for maintaining cell growth and differentiation. After cell growth, we successfully demonstrated the functionality of the myotubes with electrical stimulation which produced observable motion of the GF from the contraction of the cells. This work significantly advances the use of novel 3D scaffold materials in tissue engineering and establishes a foundation for the further investigation of engineered biological−nanomaterial interfaces.

ASSOCIATED CONTENT

Supporting Information

The Supporting Information is available free of charge on the ACS Publications website at DOI: 10.1021/acsbiomaterials.6b00139.

Figures S1−S5 (PDF)

Movie S1, time-lapse movie showing the motion cells and GF due to cell contraction triggered by an external electrical stimulus and containing the regions used for the analysis in Figure 5 (AVI)

Movie S2, time-lapse movie showing the motion of cells and GF due to cell contraction triggered by an external electrical stimulus, recorded from a separate region of the graphene than Movie S1 (AVI)

AUTHOR INFORMATION

Corresponding Author

*E-mail: daveestrada@boisestate.edu.

DOI: 10.1021/acsbiomaterials.6b00139
ACS Biomater. Sci. Eng. 2016, 2, 1234−1241

Present Address
‡E.K. is currently at Department of Chemical and Biomolecular Engineering, Lehigh University, 111 Research Drive, Bethlehem, PA 18015, United States

Notes
The authors declare no competing financial interest.

■ ACKNOWLEDGMENTS

The MHC antibody, developed by D.A. Fischman, was obtained from the Developmental Studies Hybridoma Bank, created by the National Institute of Child Health and Human Development of the National Institutes of Health and maintained at The University of Iowa, Department of Biology, Iowa City, IA 52242. Research reported in this publication was supported by Institutional Development Awards (IDeA) from the National Institute of General Medical Sciences of the National Institutes of Health under grant numbers P20GM103408 and P20GM109095. We also acknowledge support from the Biomolecular Research Center at Boise State University with funding from the National Science Foundation, Grant 0619793 and 0923535, the MJ Murdock Charitable Trust, and the Idaho State Board of Education. We thank Dr. Piyush Bajaj and Dr. Rashi Iyer for helpful discussions and Barb Jibben for editorial services. The content is solely the responsibility of the authors and does not necessarily represent the official views of the National Institutes of Health. Additionally, the authors acknowledge the generous startup funding provided by the Micron School of Materials Science and Engineering at Boise State University.

■ REFERENCES

(1) Bajaj, P.; Schweller, R. M.; Khademhosseini, A.; West, J. L.; Bashir, R. 3D Biofabrication Strategies for Tissue Engineering and Regenerative Medicine. *Annu. Rev. Biomed. Eng.* **2014**, *16*, 247−276.
(2) Huh, D.; Hamilton, G. a.; Ingber, D. E. From 3D cell culture to organs-on-chips. *Trends Cell Biol.* **2011**, *21*, 745−54.
(3) Kim, J. B. Three-dimensional tissue culture models in cancer biology. *Semin. Cancer Biol.* **2005**, *15*, 365−77.
(4) Lee, S. K.; Kim, H.; Shim, B. S. Graphene: an emerging material for biological tissue engineering. *Carbon Letters* **2013**, *14*, 63−75.
(5) Bajaj, P.; Rivera, J.; Marchwiany, D.; Solovyeva, V.; Bashir, R. Graphene based patterning and differentiation of C2C12 myoblasts. *Adv. Healthcare Mater.* **2014**, *3*, 995−1000.
(6) Ku, S. H.; Park, C. B. Myoblast differentiation on graphene oxide. *Biomaterials* **2013**, *34*, 2017−2023.
(7) Lee, W. C.; Lim, C. H. Y. X.; Shi, H.; Tang, L. A. L.; Wang, Y.; Lim, C. T.; Loh, K. P. Origin of Enhanced Stem Cell Growth and Differentiation on Graphene and Graphene Oxide. *ACS Nano* **2011**, *5*, 7334−7341.
(8) Nayak, T. R.; Andersen, H.; Makam, V. S.; Khaw, C.; Bae, S.; Xu, X.; Ee, P.-L. R.; Ahn, J.-H.; Hong, B. H.; Pastorin, G.; Özyilmaz, B. Graphene for controlled and accelerated osteogenic differentiation of human mesenchymal stem cells. *ACS Nano* **2011**, *5*, 4670−8.
(9) Wang, Y.; Lee, W. C.; Manga, K. K.; Ang, P. K.; Lu, J.; Liu, Y. P.; Lim, C. T.; Loh, K. P. Fluorinated graphene for promoting neuro-induction of stem cells. *Adv. Mater.* **2012**, *24*, 4285−90.
(10) Dowling, D. P.; Miller, I. S.; Ardhaoui, M.; Gallagher, W. M. Effect of Surface Wettability and Topography on the Adhesion of Osteosarcoma Cells on Plasma-modified Polystyrene. *J. Biomater. Appl.* **2011**, *26*, 327−347.
(11) Banerjee, S.; Shim, J.; Rivera, J.; Jin, X.; Estrada, D.; Solovyeva, V.; You, X.; Pak, J.; Pop, E.; Aluru, N.; Bashir, R. Electrochemistry at the Edge of a Single Graphene Layer in a Nanopore. *ACS Nano* **2013**, *7*, 834−843.
(12) Chen, Z.; Ren, W.; Gao, L.; Liu, B.; Pei, S.; Cheng, H.-M. Three-dimensional flexible and conductive interconnected graphene networks grown by chemical vapour deposition. *Nat. Mater.* **2011**, *10*, 424−428.
(13) Bong, J.; Lim, T.; Seo, K.; Kwon, C.-A.; Park, J. H.; Kwak, S. K.; Ju, S. Dynamic graphene filters for selective gas-water-oil separation. *Sci. Rep.* **2015**, *5*, 14321.
(14) Singh, E.; Chen, Z.; Houshmand, F.; Ren, W.; Peles, Y.; Cheng, H.-M.; Koratkar, N. Superhydrophobic Graphene Foams. *Small* **2013**, *9*, 75−80.
(15) Hou, J.; Shao, Y.; Ellis, M. W.; Moore, R. B.; Yi, B. Graphene-based electrochemical energy conversion and storage: fuel cells, supercapacitors and lithium ion batteries. *Phys. Chem. Chem. Phys.* **2011**, *13*, 15384−15402.
(16) Wang, W.; Guo, S.; Lee, I.; Ahmed, K.; Zhong, J.; Favors, Z.; Zaera, F.; Ozkan, M.; Ozkan, C. S. Hydrous Ruthenium Oxide Nanoparticles Anchored to Graphene and Carbon Nanotube Hybrid Foam for Supercapacitors. *Sci. Rep.* **2014**, *4*, 4452.
(17) Nieto, A.; Dua, R.; Zhang, C.; Boesl, B.; Ramaswamy, S.; Agarwal, A. Three Dimensional Graphene Foam/Polymer Hybrid as a High Strength Biocompatible Scaffold. *Adv. Funct. Mater.* **2015**, *25*, 3916−3924.
(18) Samad, Y. A.; Li, Y.; Alhassan, S. M.; Liao, K. Novel Graphene Foam Composite with Adjustable Sensitivity for Sensor Applications. *ACS Appl. Mater. Interfaces* **2015**, *7*, 9195−9202.
(19) Wang, J. K.; Xiong, G. M.; Zhu, M.; Özyilmaz, B.; Castro Neto, A. H.; Tan, N. S.; Choong, C. Polymer-Enriched 3D Graphene Foams for Biomedical Applications. *ACS Appl. Mater. Interfaces* **2015**, *7*, 8275−8283.
(20) Crowder, S. W.; Prasai, D.; Rath, R.; Balikov, D. a.; Bae, H.; Bolotin, K. I.; Sung, H.-J. Three-dimensional graphene foams promote osteogenic differentiation of human mesenchymal stem cells. *Nanoscale* **2013**, *5*, 4171−6.
(21) Li, N.; Zhang, Q.; Gao, S.; Song, Q.; Huang, R.; Wang, L.; Liu, L.; Dai, J.; Tang, M.; Cheng, G. Three-dimensional graphene foam as a biocompatible and conductive scaffold for neural stem cells. *Sci. Rep.* **2013**, *3*, 1604.
(22) Cvetkovic, C.; Raman, R.; Chan, V.; Williams, B. J.; Tolish, M.; Bajaj, P.; Sakar, M. S.; Asada, H. H.; Saif, M. T. A.; Bashir, R. Three-dimensionally printed biological machines powered by skeletal muscle. *Proc. Natl. Acad. Sci. U. S. A.* **2014**, *111*, 10125−10130.
(23) Schneider, C. A.; Rasband, W. S.; Eliceiri, K. W. NIH Image to ImageJ: 25 years of image analysis. *Nat. Methods* **2012**, *9*, 671−675.
(24) Marotta, M.; Bragos, R.; Gomez-Foix, A. M. Design and performance of an electrical stimulator for long-term contraction of cultured muscle cells. *BioTechniques* **2004**, *36*, 68−73.
(25) Meijering, E.; Dzyubachyk, O.; Smal, I. Methods for Cell and Particle Tracking. In *Methods in Enzymology*; Academic Press: New York, 2012; Vol. *504*, chapter 9, pp 183−200. DOI: http://dx.doi.org/10.1016/B978-0-12-391857-4.00009-4.
(26) Nieto, A.; Boesl, B.; Agarwal, A. Multi-scale intrinsic deformation mechanisms of 3D graphene foam. *Carbon* **2015**, *85*, 299−308.
(27) Engler, A. J.; Griffin, M. A.; Sen, S.; Bönnemann, C. G.; Sweeney, H. L.; Discher, D. E. Myotubes differentiate optimally on substrates with tissue-like stiffness pathological implications for soft or stiff microenvironments. *J. Cell Biol.* **2004**, *166*, 877−887.
(28) Lu, H.; Shah, P.; Ennis, D.; Shinder, G.; Sap, J.; Le-Tien, H.; Fantus, I. G. The Differentiation of Skeletal Muscle Cells Involves a Protein-tyrosine Phosphatase-α-mediated C-Src Signaling Pathway. *J. Biol. Chem.* **2002**, *277*, 46687−46695.
(29) Filigheddu, N.; Gnocchi, V. F.; Coscia, M.; Cappelli, M.; Porporato, P. E.; Taulli, R.; Traini, S.; Baldanzi, G.; Chianale, F.; Cutrupi, S.; Arnoletti, E.; Ghè, C.; Fubini, A.; Surico, N.; Sinigaglia, F.; Ponzetto, C.; Muccioli, G.; Crepaldi, T.; Graziani, A. Ghrelin and Des-Acyl Ghrelin Promote Differentiation and Fusion of C2C12 Skeletal Muscle Cells. *Mol. Biol. Cell* **2007**, *18*, 986−994.
(30) Bajaj, P.; Reddy, B.; Millet, L.; Wei, C.; Zorlutuna, P.; Bao, G.; Bashir, R. Patterning the differentiation of C2C12 skeletal myoblasts. *Integrative Biology* **2011**, *3*, 897−909.

DOI: 10.1021/acsbiomaterials.6b00139
ACS Biomater. Sci. Eng. 2016, 2, 1234−1241

(31) Burattini, S.; Ferri, P.; Battistelli, M.; Curci, R.; Luchetti, F.; Falcieri, E. C2C12 murine myoblasts and a model ok skeletal muscle development: morpho-functional characterization. *Eur. J. Histochem.* **2004**, *48*, 223−234.
(32) Miyake, T.; McDermott, J. C.; Gramolini, A. O. A Method for the Direct Identification of Differentiating Muscle Cells by a Fluorescent Mitochondrial Dye. *PLoS One* **2011**, *6*, e28628.
(33) Andres, V.; Walsh, K. Myogenin Expression, Cell Cycle Withdrawal, and Phenotypic Differentiation Are Temporally Separable Events that Precede Cell Fusion upon Myogenesis. *J. Cell Biol.* **1996**, *132*, 657−666.
(34) Park, H.; Bhalla, R.; Saigal, R.; Radisic, M.; Watson, N.; Langer, R.; Vunjak-Novakovic, G. Effects of electrical stimulation in C2C12 muscle constructs. *J. Tissue Eng. Regener. Med.* **2008**, *2*, 279−287.
(35) Ishibashi, T.; Hoshino, Y.; Kaji, H.; Kanzaki, M.; Sato, M.; Nishizawa, M. Localized electrical stimulation to C2C12 myotubes cultured on a porous membrane-based substrate. *Biomed. Microdevices* **2009**, *11*, 413−419.
(36) Fujita, H.; Nedachi, T.; Kanzaki, M. Accelerated de novo sarcomere assembly by electric pulse stimulation in C2C12 myotubes. *Exp. Cell Res.* **2007**, *313*, 1853−1865.
(37) Hidalgo-Bastida, L. A.; Cartmell, S. H. Mesenchymal stem cells, osteoblasts and extracellular matrix proteins: enhancing cell adhesion and differentiation for bone tissue engineering. *Tissue Eng., Part B* **2010**, *16*, 405−412.
(38) McCarthy, J.; Basara, M.; Palm, S.; Sas, D.; Furcht, L. The role of cell adhesion proteins—laminin and fibronectin—in the movement of malignant and metastatic cells. *Cancer Metastasis Rev.* **1985**, *4*, 125−152.
(39) Bougas, K.; Stenport, V. F.; Tengvall, P.; Currie, F.; Wennerberg, A. Laminin Coating Promotes Calcium Phosphate Precipitation on Titanium Discs *in vitro*. *J. Oral Maxillofacial Res.* **2011**, *2*, e5.
(40) Bozkurt, A.; McConnell, G. C. Bionanotechnological Advances in Neural Recording and Stimulation. In *Novel Advances in Microsystems Technologies and Their Applications*; Francis, L. A., Iniewski, K., Eds.; CRC Press: Boca Raton, FL, 2013; pp 437−460.
(41) Rakhilin, S.; Turner, G.; Katz, M.; Warden, R.; Irelan, J.; Abassi, Y. A.; Glass, D. J. Electrical Impedance as a Novel Biomarker of Myotube Atrophy and Hypertrophy. *J. Biomol. Screening* **2011**, *16*, 565−574.
(42) Engler, A. J.; Sen, S.; Sweeney, H. L.; Discher, D. E. Matrix elasticity directs stem cell lineage specification. *Cell* **2006**, *126*, 677−689.

DOI: 10.1021/acsbiomaterials.6b00139
ACS Biomater. Sci. Eng. 2016, 2, 1234−1241

Supporting Information

Graphene Foam as a 3D Platform for Myotube Growth

Eric Krueger[1†], A. Nicole Chang[1], Dale Brown[1], Josh Eixenberger[2,3], Raquel Brown[2], Sepideh Rastegar[4], Katie M. Yocham[5], Kurtis D. Cantley[4], David Estrada[1]*

[1]Micron School of Materials Science and Engineering, [2]Biomolecular Research Center, [3]Physics Department, [4]Department of Electrical and Computer Engineering, [5]Department of Mechanical and Biomedical Engineering, Boise State University, 1910 University Dr., Boise, ID 83725, United States

*Email: daveestrada@boisestate.edu

†*Current Address: Department of Chemical and Biomolecular Engineering, Lehigh University, 111 Research Dr., Bethlehem, PA 18015, United States*

Number of Pages: 5

Number of Figures: 5

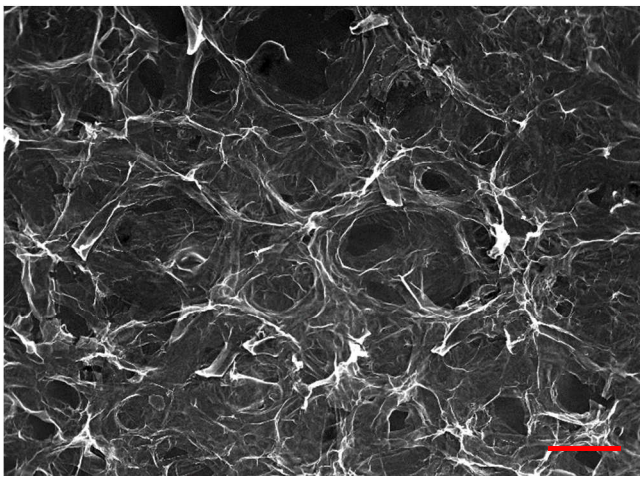

Figure S1. SEM image of GF after etching Ni foam. Scale bar: 200 μm.

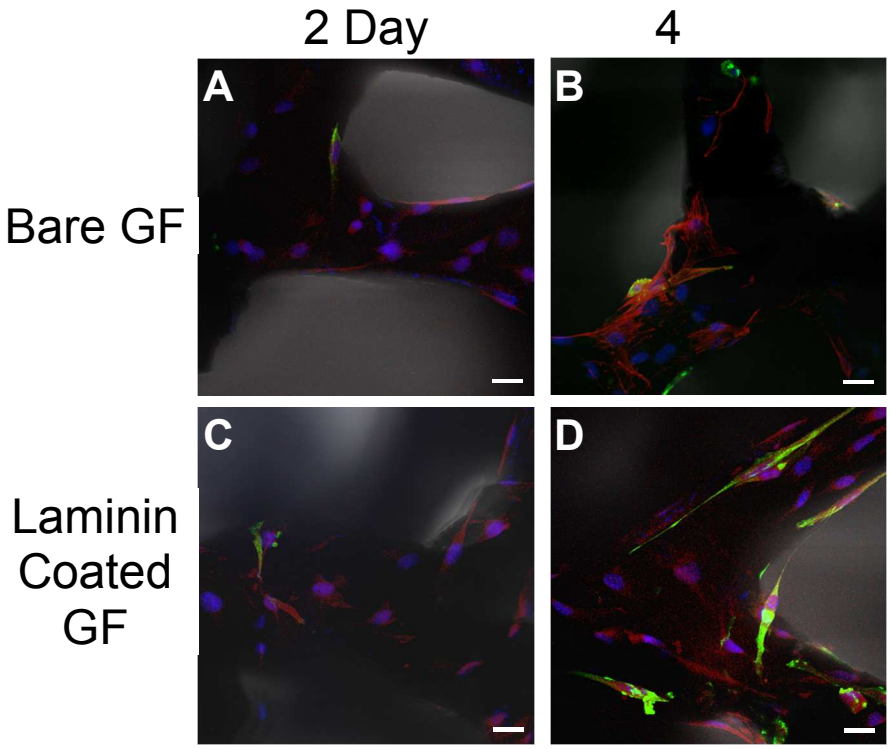

Figure S2. Additional confocal Z-stack images of C2C12 cells cultured on GF. Blue, nuclei (Hoechst); red, actin (Alexa Fluor 546 phalloidin) Green, MF-20 (Alexa Fluor 488 goat anti-mouse) (A) Growth on bare GF after culture in DM for 2 days and (B) 4 days. (C) Laminin coated GF after cultured in DM for 2 days and (D) 4 days. Scale bars: 20 μm.

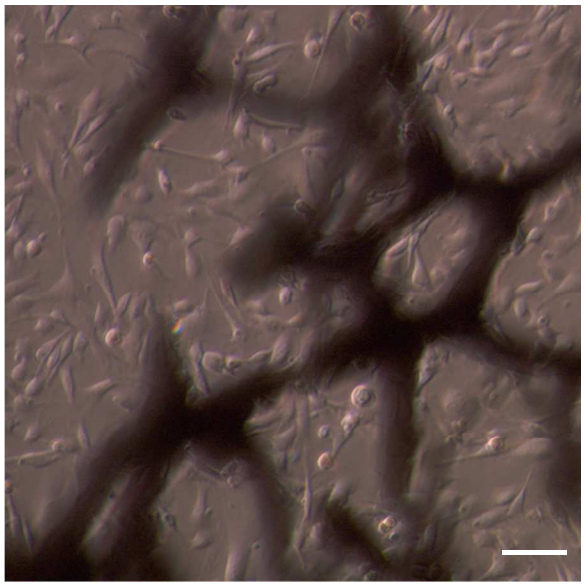

Figure S3. Optical microscopy image showing C2C12 cells 24 hours after seeding the GF. C2C12 seeds that do not adhere to the graphene foam during seeding can be seen on the bottom of the cell culture dish. Scale bar: 100 μm.

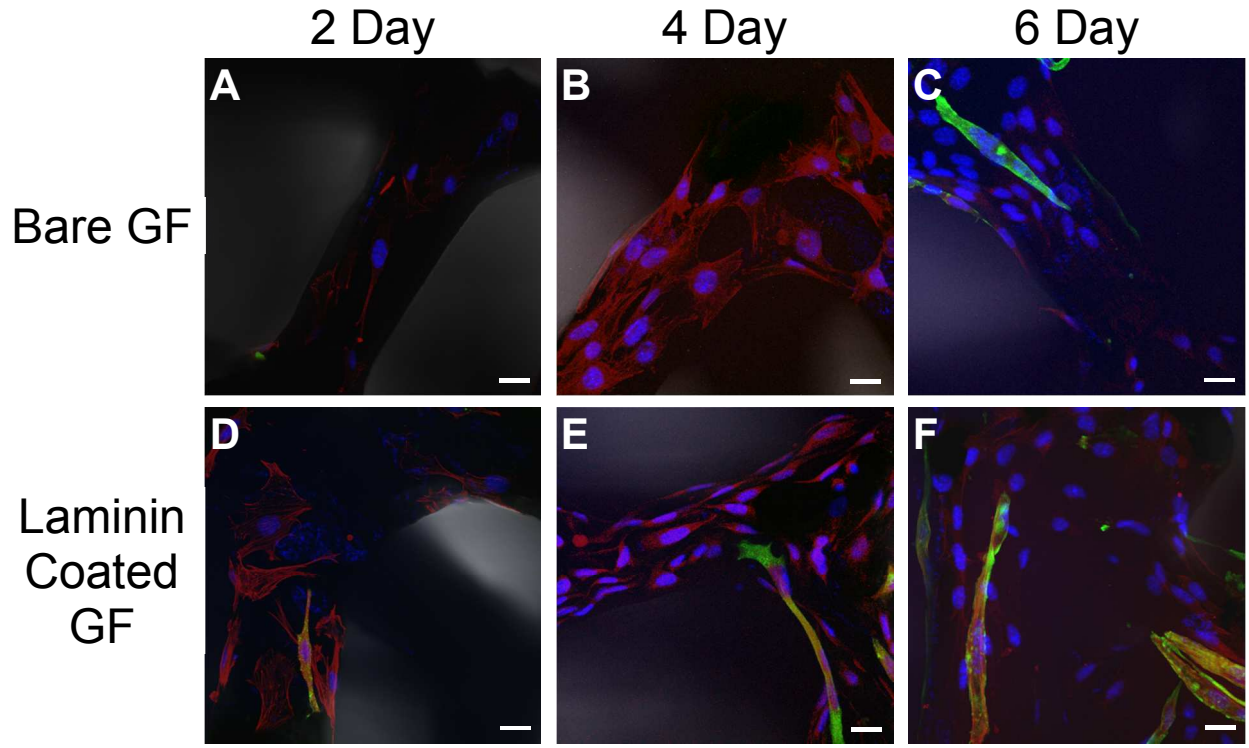

Figure S4. Representative confocal z-stack images of C2C12 cells cultured on GF. Blue, nuclei (Hoechst); red, actin (Alexa Fluor 546 phalloidin); Green, MF-20 (Alexa Fluor 488 goat anti-mouse) (A) Growth on bare GF after culture in DM for 2 days, (B) 4 days, (C) 6 days. (D) Laminin coated GF after cultured in DM for 2 days, (E) 4 days, (F) 6 days. Scale bars: 20 μm.

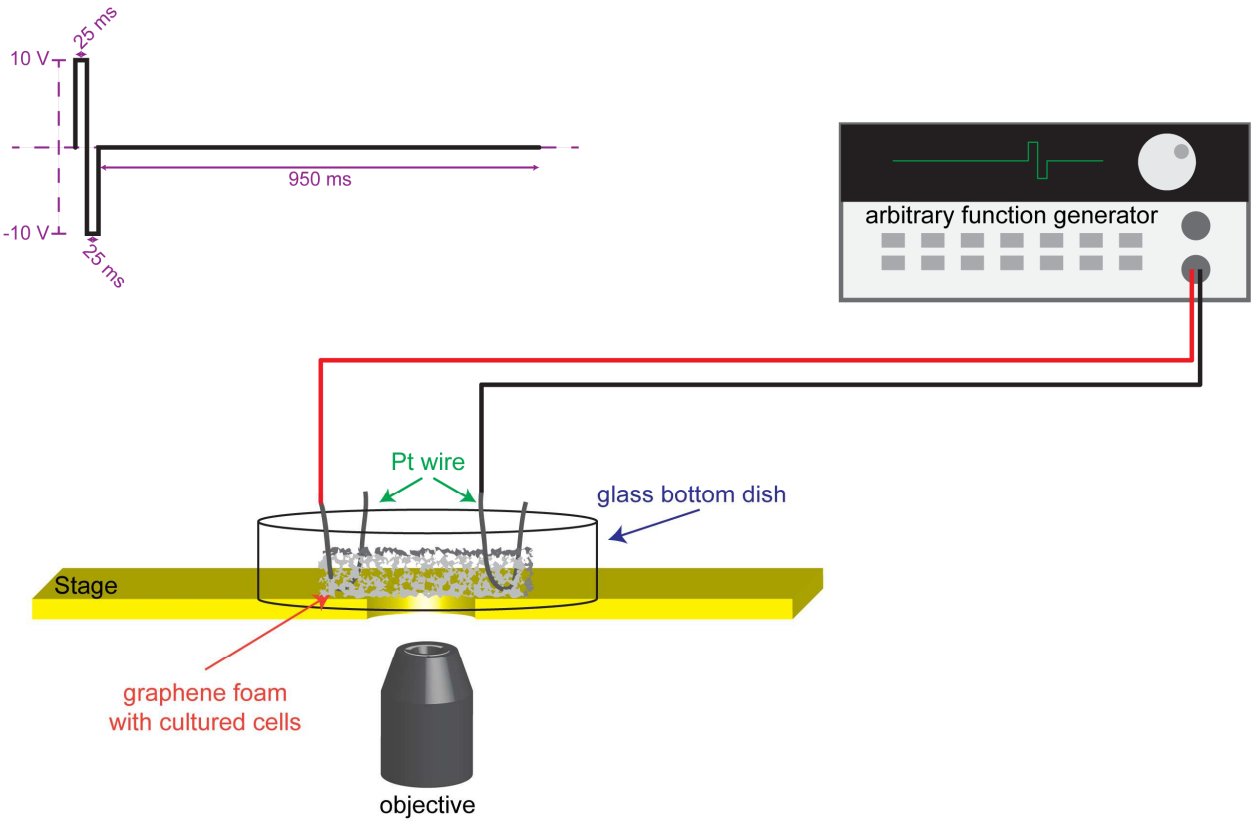

Figure S5. A schematic of the experimental setup for cell/GF electrical stimulation. Drawing not to scale.